

Sex-specific effects of acetylation on tauopathy in aging htau mice

Received: 3 November 2025

Accepted: 23 February 2026

Published online: 03 March 2026

Cite this article as: Sabir U., Csubak B.A., Ilchenko S. *et al.* Sex-specific effects of acetylation on tauopathy in aging htau mice. *Sci Rep* (2026). <https://doi.org/10.1038/s41598-026-41691-0>

Usman Sabir, Bovinari Alistair Csubak, Serguei Ilchenko, Mohammad Yunus Ansari, Nicholas M. Kanaan, Tsung-Heng Tsai, Dasarathy Srinivasan, Christine M. Dengler-Crish & Takhar Kasumov

We are providing an unedited version of this manuscript to give early access to its findings. Before final publication, the manuscript will undergo further editing. Please note there may be errors present which affect the content, and all legal disclaimers apply.

If this paper is publishing under a Transparent Peer Review model then Peer Review reports will publish with the final article.

ARTICLE IN PRESS

Sex-specific effects of acetylation on tauopathy in aging htau mice

Usman Sabir¹, Bovinari Alistair Csubak¹, Serguei Ilchenko¹, Mohammad Yunus Ansari², Nicholas M. Kanaan³, Tsung-Heng Tsai⁴, Dasarathy Srinivasan⁵, Christine M. Dengler-Crish¹, Takhar Kasumov¹.

¹Department of Pharmaceutical Sciences, College of Pharmacy, Northeast Ohio Medical University, Rootstown, OH 44272

²Department of Biomedical Sciences, College of Medicine, Northeast Ohio Medical University, Rootstown, OH 44272

³Department of Translational Neuroscience, College of Human Medicine, Michigan State University, Grand Rapids, MI 49503, USA

⁴Department of Mathematical Sciences, Kent State University, Kent, OH 44242

⁵Departments of Inflammation and Immunity and Gastroenterology/Hepatology, Northern Ohio Alcohol Center, Cleveland Clinic, Cleveland, OH 44195

Corresponding authors:

Christine M. Dengler-Crish

Tel 330-325-6598; Fax 409-772-9670; email: ccrish@neomed.edu

Takhar Kasumov, Ph.D.

Tel 330-325-6552; Fax 409-772-9670; email: tkasumov@neomed.edu

Running title: Sex-specific tauopathy in htau mice

Abstract

Alzheimer's disease involves extracellular β -amyloid accumulation and intracellular phosphorylated tau aggregates, with higher disease prevalence and neuropathological burden in aging females. While tau phosphorylation contributes to tau pathology, other modifications, such as acetylation, also promote aggregation. Aging disrupts proteostasis, in part through acetylation, a post-translational modification affecting protein function and stability; however, its role in sex-specific tauopathy remains unclear.

This study investigated acetylation in an age-, sex-specific manner across presymptomatic (3-5 months), progressive (11-14 months), and advanced (>16 months) stages of tauopathy in htau mice using immunoassays. In females, cortical tau K174 acetylation increased with age and disease progression, correlating with tau accumulation. In males, tau phosphorylation increased without acetylation changes, indicating sex-specific regulation. Free ubiquitin, a marker of impaired proteasomal degradation, rose with age in both females and males. Autophagy markers also showed marked age-related decline in both sexes, contributing to tau accumulation. Increased mTOR expression in aged mice further suggested mTOR-driven autophagy inhibition.

These findings suggest that aging-related disruptions in brain acetylation are associated with accelerated tau pathology, with females potentially being more vulnerable due to elevated tau acetylation coinciding with impaired protein degradation pathways.

Keywords: tauopathy, acetylation, phosphorylation, oligomers, autophagy

INTRODUCTION

Alzheimer's disease (AD), the leading cause of dementia and a major global health challenge, is a progressive neurodegenerative disorder characterized by cognitive decline and memory loss. [1-3]. While aging is the primary risk factor for AD, nearly two-thirds of those diagnosed with AD are females [4, 5], underscoring the need to understand sex-related mechanisms. Pathologically, AD is marked by extracellular β -amyloid ($A\beta$) accumulation and intracellular neurofibrillary tangles (NFTs) formed from tau aggregation [6]. While $A\beta$ amelioration has long been a therapeutic focus, these efforts do not entirely address tauopathy, which more closely correlates with neurodegeneration and cognitive decline [7]. Tau dysfunction is also a central feature of a broader spectrum of neurodegenerative disorders, including frontotemporal dementia (FTD), progressive supranuclear palsy (PSP), corticobasal degeneration (CBD), and chronic traumatic encephalopathy (CTE) [8]. Recent studies using the K3 tauopathy mouse model revealed a sex-specific response to tau immunotherapy, with significant efficacy in females but not males [9], highlighting the importance of investigating sex-specific mechanisms to inform targeted treatment strategies across tauopathies.

Tau protein plays a critical role in numerous cellular processes, most notably in binding to and regulating the dynamics of microtubules [10]. Tauopathy involves the formation of aggregates from irregular post-translational modifications (PTMs) of tau, including hyperacetylation and hyperphosphorylation [11, 12]. The human brain produces six main tau isoforms via alternative splicing of a single gene, classified as three-repeat (3R) or four-repeat (4R) forms depending on exon 10 inclusion [13, 14]. In healthy individuals, these isoforms are expressed at roughly equal levels but in tauopathies the homeostatic balance is disrupted [15, 16]. The tau protein consists of an acidic *N*-terminal region, followed by a basic proline-rich region (PRR, amino acids 151-243), and a basic *C*-terminal tail. This arrangement creates a dipole structure with oppositely charged domains that can be modulated by PTMs. The microtubule-binding regions (MTBR) of tau (R1-R4), spanning amino acids 244 to 368 near the *C*-terminus, are critical for its function [17]. Positively charged lysine residues in these regions interact with negatively charged components of microtubules, regulating their dynamics and supporting neuronal differentiation, axonal transport, and synaptic function. Notably, the unmodified PRR of tau is intrinsically disordered due to electrostatic repulsion between positively charged lysine residues, which helps to maintain tau in non-aggregated state [18].

Physiological tau functions are maintained through cellular proteostasis mechanisms, including synthesis, folding, PTMs, and degradation [19-21]. Abnormal modifications may disrupt tau proteostasis and contribute to conformational changes and tau aggregation, one of the earliest alterations of tau in AD [22]. Emerging evidence indicates that tau oligomers, pre-fibrillar multimers, are more neurotoxic and pathologically relevant than mature fibrillar aggregates [23]. Granular tau oligomers have been biochemically isolated and detected at very early stages of AD, preceding clinical symptoms and the formation of NFT [24]. Several forms of pathogenic tau, including abnormal conformations, impair axonal transport [25] and may lead to disrupted mitochondrial distribution and altered dynamics of mitochondrial fusion and fission [26]. Unlike other tauopathies such as Pick's disease and FTD, AD-associated tau aggregates predominantly involve 3R or 4R isoforms and primarily affect different cell types that impact memory and cognition [27]. Although tau phosphorylation is

widely believed to facilitate oligomerization [28], the mechanisms underlying phosphorylation-independent tau aggregation, particularly in non-mutant, wild-type tau, remain poorly understood.

Beyond phosphorylation, dysregulated ϵ -lysine acetylation is implicated in several neurodegenerative diseases, including AD. Recent cryogenic electron microscopy (cryo-EM) of NFT indicates acetylation as a key structural determinant of NFT [29]. Additionally, emerging evidence indicates that acetylation modulates tau phosphorylation and function [20, 30-32]. Elevated acetylation of tau at residues K274, K280, and K281 was observed in advanced AD [33, 34]. Accumulation of these acetylated tau species is associated with impaired synaptic plasticity and spatial memory deficits in the most common form of AD (i.e. late onset sporadic AD) [35]. Additionally, tau acetylation at lysine 174 (TauK174ac), which is detected at early stages of AD [36], is implicated in promoting tau aggregation [21]. Recent studies suggest that reducing neuronal TauK174ac is neuroprotective following traumatic brain injury (TBI) in mice and may also protect against AD progression post-TBI [37]. Notably, treatment with anti-TauK174ac antibodies attenuates tau pathology and improves cognitive function in PS19 mice, a model of P301S mutation-driven tauopathy linked to frontotemporal lobar degeneration [10]. These data show TauK174ac as a promising therapeutic target for tauopathies, including AD.

To investigate the role of acetylation in sex-dependent and A β -independent tauopathy progression, we characterized site-specific tau acetylation, along with tau phosphorylation and oligomerization, in male and female htau mice of different ages and examined their associations with sex-specific patterns of tau accumulation and autophagy-related changes.

Materials and methods

Animal experiments. All animal procedures were approved by the Northeast Ohio Medical University (NEOMED) Institutional Animal Care and Use Committee (IACUC; approval date: February 26, 2025; protocol no. 25-01-417) and conducted according to the Guidelines for the Care and Use of Laboratory Animals (National Institutes of Health publication no. 85-23). Reporting of this animal research complies with the ARRIVE guidelines (<https://arriveguidelines.org>).

Htau mice (Jax# 005491, C57BL/6J background) were used for the experiments in this study. These mice express all six human tau isoforms and lack endogenous mouse tau, making it suitable for modeling human tauopathy. The strain was originally generated by crossing 8c transgenic mice [38], which carry a human tau transgene derived from a P1-derived artificial chromosome (PAC) construct, with tau knockout ($\tau^{-/-}$) mice lacking exon 1 of the *Mapt* gene [39]. Mice were bred in-house and htau genotyping was performed via polymerase chain reaction using primers specific for the human tau transgene, the mouse *Mapt* gene, and the $\tau^{-/-}$ allele (primer sequences are provided in **Supplementary Table S1**). All animals were housed in a temperature-controlled facility under a 12-hour light/dark cycle with ad libitum access to standard chow and water. At the end of each experiment, transcardiac perfusion was performed with phosphate-buffered saline (PBS) to wash out residual blood prior to brain dissection. Brain samples from $\tau^{-/-}$ mice were used as negative controls to validate tau-specific measurements in Western blot and immunoassays (**Supplementary Figure S1**).

The role of site-specific acetylation in sex dependent tauopathy progression. To examine sex- and age-dependent differences in tau acetylation, phosphorylation, and oligomerization, 24 htau mice ($n=4$ per sex and age group) were analyzed across three tauopathy stages: young (3–5 months, presymptomatic), middle-aged (11–14 months, progressive), and old (>16 months, symptomatic). Young males exhibited modestly higher body weight compared with age-matched females (27.8 ± 2.9 g vs 22.9 ± 1.8 g, $p = 0.047$). Body weight increased in both sexes at middle age, with no significant sex difference (34.0 ± 2.8 g vs 30.9 ± 1.0 g; $p > 0.05$). At advanced ages, body weight plateaued; however, males remained significantly heavier than females (36.4 ± 3.1 g vs 29.2 ± 3.2 g; $p < 0.05$). After perfusion with PBS, the hippocampus and prefrontal cortex were rapidly dissected, freeze-clamped, and stored at -80°C for biochemical analyses. Given its central role in tau pathology, the prefrontal cortex was specifically examined for age- and sex-related changes. An additional cohort of 19-month-old male and female mice ($n = 4$ per group) was used for terminal immunofluorescence studies.

Immunoblot analysis. Proteins from the pre-frontal cortex region of the brain homogenate were extracted using the total protein extraction reagent (TPER buffer, 25 mM bicine 150 mM sodium chloride, pH 7.6, ThermoFisher Scientific, Waltham MA; Cat# 78510) supplemented with protease (A32963), phosphatase (A32957), and deacetylase inhibitors (5 μM trichostatin). Equal protein amounts (15–30 μg) were separated on 4–20% gradient sodium dodecyl sulfate-polyacrylamide gel electrophoresis (SDS-PAGE) gels (Bio-Rad, Hercules, CA) at 120 V for 120 min and then electro-transferred to polyvinylidene difluoride membranes at 100 V for 60 min. The membranes were incubated with primary anti-Tau (Tau12; BioLegend, cat# 806501, RRID: AB_2564707; [40, 41]), anti-pTau S202/Th205 (AT8 antibody; 1:100; Invitrogen #MN1020, RRID: AB_223647), anti-pTauTh231 (Signalway Antibody, cat#

13381), and anti-TauK174Ac (CreativeBiolabs # MOB621CQ,) antibodies overnight at 4°C, (details are provided in **Supplementary table S2**). Subsequently, membranes were incubated for 1 hour at room temperature with a 1:3000 diluted HRP-conjugated anti-mouse IgG secondary antibody (Cell signaling, 7076P2, RRID: AB_330924). Finally, detection procedures were performed using the FluorChem imager. Band intensities were measured by the Alphaview software (Version 3.4.0.0, ProteinSimple, San Jose, CA). Human tau-specific antibodies were validated by using tau^{-/-} and wild type C57BL/6j mice (**Supplementary Figure S1A-D**). Vendors validated all other antibodies.

Dot blot analysis of tau oligomers. Oligomeric tau was detected using the Tau Oligomeric Complex 1 (TOC1) antibody (Kanaan Lab; AB_2832939), which was originally generated against purified recombinant cross-linked tau dimers [42, 43]. TOC1 recognizes a continuous epitope located within amino acids 209–224 in the PRR of tau. This antibody is conformation-dependent: its epitope is accessible in tau oligomers and dimers but concealed in monomeric and filamentous tau forms. Consequently, tau oligomerization was assessed using nondenaturing dot blot assays, where signals were normalized to total tau levels. Proteins from prefrontal cortex homogenates were extracted using ThermoFisher TPER buffer (Cat# 78510) without detergents, supplemented with protease (A32963), phosphatase (A32957,) minitabets, and deacetylase inhibitors (trichostatin, 5 μM). Tissue-to-buffer ratio was 1:20 (1 mg tissue in 20 μL buffer). Samples were sonicated at 10% amplitude with 3s ON/OFF pulses. Three μl of each sample (3 μg protein) was spotted onto a 0.22 μm nitrocellulose membrane (BIORAD, Cat# 1620097). After drying, the membrane was blocked with 5% non-fat dry milk in 1X TBS-T (0.5%, pH 7.4) for 30 min. The TOC1 antibody was diluted 1:8000 in tris-buffered saline with tween 20 (TBS-T) and incubated overnight at 4°C. The membrane was then rinsed and incubated with HRP-conjugated anti-mouse secondary antibody (same as above) for 1 hour. After three 15-minute washes, the membrane was imaged using a ProteinSimple FluorChem system with enhanced chemiluminescence (ECL) reagent (BIORAD). Dot intensities were quantified using AlphaView software (v3.4.0.0). Total tau normalization was performed by detecting tau using the pan-tau antibody Tau12. Protein loading was normalized using total protein detection with 0.1% Ponceau staining.

Immunofluorescent labeling of neuropathology in htau mice. To assess tau pathology, formalin-fixed brain tissues were processed using multichannel immunofluorescence to co-label acetylation, phosphorylation, cell-type, and inflammatory markers. Mice were euthanized with sodium pentobarbital, followed by transcardiac perfusion with 4% paraformaldehyde in PBS. After cryoprotection in 20% sucrose/PBS, 50 μm hippocampal sections spanning the entire brain were cut using a freezing-stage microtome.

Immunofluorescence staining was performed at 37°C: tissue sections were blocked with donkey serum for 30 minutes, incubated with primary antibodies for 1 hour, washed three times in PBS, and then incubated with Alexa Fluor-conjugated secondary antibodies (dilution: 1:200) for 60 minutes. After additional washes, slides were mounted with Fluoromount-G. Primary antibodies targeted TauK174ac (1:100) and pTauS202/Thr205 (AT8) to label acetylated and phosphorylated tau, respectively, NeuN (1:500; SYSY #266004, RRID: AB_2619988) as a neuronal marker, and Ionized Calcium-Binding Adapter Molecule 1 (Iba1; 1:1000; Abcam #ab5076, RRID: AB_2224402) as a microglia marker since tau pathology is associated with

neuroinflammation and microglial activation [44, 45]. Tau acetylation at lysine 174 site is an early biomarker in AD and a key regulator of tau homeostasis and cognitive deficits in mice [21]. In AD and other tauopathies, pathological tau inclusions are immunoreactive to the AT8 antibody, which detects phosphorylation at S202/Th205 and S208 site throughout disease stages [46, 47].

Sections were imaged using a Zeiss AxioZoom V16 epifluorescent microscope equipped with 4-channel epifluorescent capability, a digital high-resolution camera, computer-guided motorized Z and X-Y stage, and Zen 2.6 software with tiling and extended depth of focus modules [48]. Images were z-stacked (~12-18 sections in z-plane per region) and orthogonal views were generated within Zen software to identify co-localization of pTauS202 and TauK174ac within cells. Extended depth of focus module was used to flat z-stack images for presentation. Fiji/ImageJ software was used to quantify total fluorescence signal from both acetylated tau and ptau202 positive puncta across threshold-calibrated hippocampal sections were measured and divided by the total area of each dentate gyrus hemifield to produce the variable of integrated fluorescence density for female and male htau mice. To determine the level of colabel between acetylated tau and ptau202, Manders' coefficients (M2) were derived using the JaCOP plug-in for Fiji/ImageJ software by simultaneously comparing individual sections of unflattened z-stack images with merged label to determine the percentage of overlap between the two different label patterns [49].

Statistical analysis. Actin was used as a loading control to normalize band intensities, ensuring accurate quantification of target protein levels. A two-way analysis of variance (ANOVA) was used to assess the main effects of sex (two levels: male and female), age (three levels: young, middle-aged, and old), and their interaction on the expression level of each marker. When a significant sex \times age interaction was detected (F-test $p < 0.05$), post hoc interaction analyses were conducted by testing three age contrasts (old vs. young, old vs. middle-aged, and middle-aged vs. young) within each sex, as well as sex contrasts within each age group. When the interaction term was not significant, the main effect of age was evaluated, and if significant ($p < 0.05$), post hoc comparisons among the three age groups were performed while collapsing across sex. Post hoc analyses were carried out using the estimated marginal means (EMMs) framework [50], as implemented in the emmeans R package [51]. Bonferroni correction was applied to adjust for multiple comparisons. In addition to marker-specific analyses, Pearson correlation coefficients were calculated for all pairs of quantified markers to explore potential associations between markers. The statistical analyses were performed using R (version 4.5.2).

Results

Age- and sex-dependent changes in tau acetylation at lysine 174 (TauK174ac) in htau mice. To investigate the contribution of TauK174ac to age-related, sex-specific tau oligomerization, we performed immunohistochemistry on hippocampal dentate gyrus (specifically targeting polymorph region or DGpo) hemifields, an important area of hippocampus involved in memory formation and spatial navigation, from symptomatic age (19-month-old) female and male (htau mice, and tau^{-/-} controls (**Figure 1**). Both sexes exhibited increased phosphorylated tau with age, but females showed greater distribution of TauK174ac throughout the DGpo region. Although both acetylated tau and phosphorylated tau were expressed in this region, there was negligible overlap in expression (**Supplementary Figure S2**). Two-sample t-tests revealed that female mice exhibited significantly greater fluorescence signal for TauK174ac ($p = 0.020$) and ptauS202/Th205 ($p = 0.006$) compared to their male htau counterparts (Figure 1 bar graphs). Females also exhibited significantly greater colabeling (i.e. higher Manders Coefficients) than males ($p = 0.020$). Immunofluorescence further demonstrated heightened microglial activation coinciding with TauK174ac in females (**Figure 2**). No signals were detected in tau^{-/-} controls. Together, these data suggest that while phosphorylated tau accumulates with age in both sexes, elevated TauK174ac and inflammation are female specific.

To further investigate the role of TauK174ac in sex-specific, age-dependent tauopathy, we quantified its expression alongside tau phosphorylation (pTauS202/Th205, pTauTh231), total tau (Tau12) levels, and tau oligomers (TOC1) in the prefrontal cortex of female and male mice using site-specific antibodies across different age groups: young (3–4 months), middle-aged (11–14 months), and old (16–19 months). Baseline levels of acetylated, phosphorylated, total, and oligomeric tau did not differ between sexes or age groups (**Figure 3A-C, Supplementary Figure S3A-E**, and Supplementary Table 3B; all $p > 0.05$). However, two-way ANOVA revealed distinct age- and sex-dependent patterns in total tau and tau post-translational modifications.

Total tau (Tau12) levels showed a significant sex \times age interaction ($p < 0.05$; **Figure 3A-C and Supplementary Table 3A**). Levels remained stable across age in males, whereas females exhibited a significant increase at advanced age compared with younger females (3–5 vs. ≥ 16 months, adjusted $p < 0.05$). In contrast, tau phosphorylation exhibited a different pattern: pTauS202/Th205 (AT8) increased significantly with aging in males (3–5 months vs. 16+ months, adjusted $p = 0.008$), whereas phosphorylation changes in females were not significant (**Figure 3B&C and Supplementary Table 3B**). Based on visual inspection (**Figure 3A&B**), TauK174ac appears to exhibit opposite age-related trends by sex: quantified intensities increased over time in female mice (**Figure 3C, last bar graph**). This pattern is supported by a significant sex \times age interaction (**Supplementary Table 3A** $p = 0.006$). Post hoc analyses of the interaction effects were consistent with this observation, although the estimated age-group differences did not remain significant after Bonferroni correction (e.g., adjusted $p = 0.0692$ for the increase from 3–5M to 16+M in females, **Supplementary Table 3B**). Consistent with prior reports [52], TOC1-positive tau oligomers, a marker associated with tau pathology, increased with age in both males and females (**Figure 3D-F**). Although **Figure 3F** suggests a greater magnitude of TOC1 accumulation in females than in males, the sex \times age interaction

was not significant ($p = 0.578$). Post hoc comparisons of the main age effect confirmed a significant increase from 3–5 months to ≥ 16 months (adjusted $p = 0.006$). Collectively, these findings indicate that age-dependent tau aggregation increases in the cortex of both male and female htau mice. In contrast, females exhibited higher levels of total tau and tau acetylation, whereas males showed relatively greater tau phosphorylation, indicating distinct, sex-dependent patterns of tau post-translational modifications associated with tau accumulation and aggregation.

Age- and sex-dependent changes in CBP/p300 and tau acetylation-related pathways. Acetylation is dynamically regulated by acetyl-CoA-dependent lysine acetyl transferases (KATs) and NAD⁺-dependent sirtuins (**Figure 4A**). To understand sex-dependent acetylation changes in htau mice, we assessed the expression of KATs, deacetylases, and key enzymes involved in nuclear-cytosolic acetyl-CoA production. CREB-binding protein (CBP) and E1A-binding protein p300 (p300) are well-established regulators of tau acetylation and are implicated in AD pathology [21]. Increased CBP/p300 activity enhances tau acetylation and promotes tau accumulation, whereas its pharmacological inhibition reduces tau burden [30]. NAD⁺-dependent sirtuins SIRT1 and SIRT6 mediate deacetylation of tau [21] and are involved in aging and AD [53].

CBP/p300 expression increased significantly with age in female htau mice but not in males, resulting in a significant sex \times age interaction ($p = 0.034$) (**Figures 4B, C, and H [top]; Supplementary Figure S4A–B**). Post hoc analyses confirmed an age-dependent increase in females that remained significant after Bonferroni correction (adjusted $p = 0.004$ for 3–5 vs. ≥ 16 months). Consistent with elevated TauK174 acetylation, CBP/p300 levels were also significantly higher in females than in males at both middle and advanced ages (adjusted $p < 0.007$ and adjusted $p = 3.8 \times 10^{-5}$, respectively, as in **Supplementary Table 3B for interactions**).

Two-way ANOVA further revealed significant sex-dependent differences in Sirt1 ($p = 4.41 \times 10^{-4}$) and Sirt6 ($p = 0.009$) expression (**Figures 4D, E, and H [middle]; Supplementary Figure S4C–D; Supplementary Table 3A for ANOVA**). However, a significant sex \times age interaction was detected only for Sirt1 ($p = 0.009$), and post hoc age-group comparisons did not remain significant after correction for multiple testing. Together, these findings indicate that although Sirt1 contributes to sex-specific regulation of tau acetylation, it is unlikely to be the primary driver of the age-dependent increase in tau acetylation observed in females. Instead, the data support a model in which enhanced lysine acetyltransferase activity, rather than reduced sirtuin-mediated deacetylation, predominantly underlies elevated tau acetylation in aged females.

The availability of acetyl-CoA influences protein acetylation [54]. Thus, we assessed enzymes involved in acetyl-CoA production, including ATP-citrate lyase (ACLY), carnitine acetyltransferase (CRAT), and acetyl-CoA synthetase 2 (ACSS2). Two-way ANOVA revealed significant main effects of sex for all three enzymes (CRAT: $p = 4.35 \times 10^{-5}$; ACLY: $p = 3.22 \times 10^{-10}$; ACSS2: $p = 1.01 \times 10^{-5}$, as in **Supplementary Table 3A**). In females, CRAT expression increased significantly from 11–14 to ≥ 16 months (adjusted $p = 0.021$), which may reflect enhanced mitochondrial acetyl-CoA export for cytosolic tau acetylation (**Figure 4F–H** (bottom left panels) **and Supplementary Figure S4E**). CRAT exhibited a significant sex \times age interaction ($p = 3.46 \times 10^{-4}$).

Post hoc analyses showed that CRAT increased from young to middle age and declined at advanced age in males, whereas females displayed a significant increase at advanced age relative to middle age. Sex comparisons revealed higher CRAT levels in males than females at middle age, with no difference at advanced age. ACLY showed a significant main effect of age ($p = 0.0237$) and a sex \times age interaction ($p = 0.047$) (**Figure 4F-G and H** (bottom right panel) **and Supplementary Figure S4F&G**). Post hoc analyses indicated that ACLY declined with age in males but remained stable across age groups in females. Despite this, ACLY levels were consistently higher in males than females at all ages. In contrast, ACSS2 did not exhibit significant age effects or a sex \times age interaction, and post hoc analyses confirmed the absence of age-dependent changes within either sex (**Supplementary Figures S4H and S5A-C**). Collectively, these results identify CRAT and ACLY, but not ACSS2, as enzymes exhibiting sex-specific, age-dependent regulation in the htau cortex and support the conclusion that elevated tau acetylation in aged females is more likely driven by increased CBP/p300 activity rather than enhanced acetyl-CoA supply.

Age- and sex-dependent alterations in autophagy- and UPS-related markers in htau mice. The ubiquitin-proteasome system (UPS) and the autophagy-lysosome pathway are the two major intracellular mechanisms for protein degradation. During the early stages of tauopathy, soluble monomeric tau is predominantly cleared by the proteasome, whereas oligomeric and aggregated tau species, which are less accessible to the UPS, are mainly degraded through autophagy [55]. Tau acetylation can enhance its stability by competing with ubiquitination at lysine residues, thereby interfering with proteasomal recognition and degradation [56].

We examined the role of UPS and autophagy in sex-dependent tauopathy. Aging did not significantly affect ubiquitinated proteins levels in female or male htau mice. In contrast, free ubiquitin levels increased progressively and significantly with age in both sexes (**Supplementary Fig. S6A-C**), consistent with acetylation-mediated inhibition of ubiquitination. The free ubiquitin accumulation may result from reduced proteasomal degradation due to impaired ubiquitination or proteolytic activity [57, 58], or from enhanced ubiquitin turnover with efficient monoubiquitin recycling [59, 60]. To evaluate UPS involvement in cortical protein accumulation, β -catenin, a canonical UPS substrate and marker of altered activity, was quantified. β -catenin levels were unchanged across ages in both sexes (**Supplementary Fig. S6D-F**), suggesting UPS-mediated proteasomal impairment is unlikely a major contributor to tauopathy in htau mice.

To investigate the role of autophagy in sex-dependent tau accumulation, we analyzed key autophagy markers, including ULK1 (unc-51-like autophagy-activating kinase, a mammalian homolog of yeast Atg1), Beclin-1, p62, Atg3, Atg5, and LC3 (microtubule-associated protein 1A/1B-light chain 3). We also quantified LAMP2A (lysosome-associated membrane protein type 2A), which regulates chaperone-mediated autophagy. ULK1 and Beclin-1 are central to autophagy initiation; regulated by mTOR (mammalian target of rapamycin)- and AMPK (AMP-activated protein kinase)-induced phosphorylation, unphosphorylated ULK1 activates autophagy by phosphorylating Beclin-1 [61] and forming a PI3K (phosphoinositide 3-kinase) complex that promotes autophagosome biogenesis [62]. Atg5 is involved in the elongation of the phagophore, which is a precursor of the autophagosome and the double-membrane

vesicles that engulf cellular components for degradation. Atg3 catalyzes the lipidation of LC3-I to LC3-II, facilitating autophagosome membrane elongation and cargo sequestration (**Figure 5A**). p62 serves as a cargo adaptor by binding ubiquitinated proteins and interacting with LC3.

The acetylation-related differences were accompanied by pronounced, pathway-specific alterations in autophagy markers. Beclin-1 remained unchanged with age or sex (**Supplementary Figure S7A, B, and C (left panel)**, and **Supplementary Figure S8A**), indicating preserved autophagosome nucleation. In contrast, ULK1 and inhibitory phosphorylation at Ser757 showed a significant age-related increase in both sexes without a sex \times age interaction (**Figure 5B-D, Supplementary Figure S8B-C, Supplementary Table 3A-C**), consistent with global, age-dependent modulation of autophagy initiation.

p62, an autophagic cargo adaptor degraded during effective flux, showed strong main effects of sex ($p = 3.1 \times 10^{-10}$) and age ($p = 0.011$), along with a significant sex \times age interaction ($p = 0.040$) (**Figure 5B-D (right panel), Supplementary Figure S8D-E, and Supplementary Table 3A**). Post hoc analyses revealed a marked accumulation of p62 in advanced-aged males, whereas females showed no age-related increase (**Supplementary Table 3B**). Moreover, males exhibited higher p62 levels than females at all ages (all $p < 3.5 \times 10^{-4}$), consistent with progressive, male-specific impairment or saturation of autophagic cargo clearance. Atg5, a key mediator of autophagosome elongation, showed a strong main effect of sex ($p = 1.2 \times 10^{-4}$) with no age or sex \times age effects (**Supplementary Table 3A; Supplementary Figure S7A-C (middle panel) and Supplementary Figure S8F**), indicating stable, sex-biased differences in basal autophagosome formation capacity across the lifespan. In contrast, Atg3, the E2-like enzyme required for LC3 lipidation, exhibited both a significant main effect of sex ($p = 5.7 \times 10^{-5}$) and a sex \times age interaction ($p = 0.0076$) (**Supplementary Table 3A**). Post hoc analyses showed a non-linear age trajectory in females, with Atg3 increasing from young to middle age and declining at advanced age, whereas males showed no age-related changes (**Supplementary Figure S7A-C (right panel), Supplementary Figure S8G and Supplementary Table 3B**). A pronounced sex difference emerged at middle age ($p = 1.5 \times 10^{-4}$), highlighting sex-specific regulation of autophagosome maturation.

Consistent with these findings, LC3-II showed a significant sex \times age interaction ($p = 0.025$) (**Figure 5E-G, Supplementary Figure S8H-I and Supplementary Table 3A**). LC3-I declined with age in both males and females ($p < 0.05$) (**Figure 5G**). The LC3-II/LC3-I ratio further showed both a main effect of sex ($p = 0.027$) and a strong sex \times age interaction ($p = 0.004$), indicating divergent regulation of autophagosome abundance and/or flux between sexes with aging.

LAMP2A, the rate-limiting lysosomal receptor for chaperone-mediated autophagy (CMA), showed a significant sex \times age interaction ($p = 0.020$) (**Figure 5H-J, Supplementary Figure S8J, and Supplementary Table 3A**). Post hoc analyses demonstrated an age-dependent increase in LAMP2A in males but not females, resulting in a significant male-female difference at advanced age ($p = 0.032$) (**Supplementary Table 3B**). This pattern suggests male-specific engagement of CMA, potentially as a compensatory response to altered macroautophagic clearance.

Collectively, these data indicate that aging does not uniformly suppress autophagy but instead reprograms autophagic pathways in a sex-dependent and phase-specific manner. While autophagy initiation signaling (ULK1) is primarily age regulated and nucleation (Beclin-1) remains stable, downstream processes, including LC3 lipidation (Atg3), autophagosome flux (LC3-II/LC3-I), cargo clearance (p62), and CMA (LAMP2A), diverge markedly between males and females. While further mechanistic studies are required, these observations raise the possibility that impaired autophagosome maturation in aged female htau mice contributes to the accumulation of acetylated and oligomeric tau, potentially linking dysregulated autophagy with tau pathology.

Role of mTORC1 and AMPK in sex-dependent tauopathy in htau mouse.

mTORC1 is a key serine/threonine kinase complex that regulates proteostasis by promoting protein synthesis and inhibiting degradation [63]. Phosphorylation at serine 2448 residue (S2448) activates mTORC1, which suppresses autophagy by phosphorylating ULK1 at S757, disrupting its interaction with and activation by AMPK, a central energy sensor [64, 65]. AMPK activation requires phosphorylation of its α -subunit at threonine 172 site (Th172) [66]. To investigate the involvement of AMPK and mTOR signaling in sex-specific tau accumulation, we quantified total and phosphorylated forms of AMPK and mTORC1 (**Figure 6A-C** and **Supplementary Figures S9A-C and Supplementary Figure S10A-H**). AMPK signaling showed no significant main effects of age or sex for pAMPK or for the pAMPK/AMPK ratio, nor any sex \times age interactions (**Supplementary Figure 9A-C**), suggesting that canonical AMPK activation and energy-sensing capacity are largely preserved across aging in both sexes. Although total AMPK protein exhibited a strong main effect of sex ($p = 1.9 \times 10^{-4}$) and a trend toward an age effect ($p = 0.061$) (**Supplementary Table 3A-C**), the absence of corresponding changes in pAMPK or pAMPK/AMPK suggests that AMPK activity per se is not dynamically altered with aging in htau mice. In contrast, mTOR signaling showed pronounced age- and sex-dependent regulation (**Figure 6A-C** and **Supplementary Table 3A-C**). Both p-mTOR and the p-mTOR/mTOR ratio exhibited significant sex \times age interactions ($p = 0.0073$ and $p = 0.010$, respectively). Post hoc analyses revealed a transient increase in p-mTOR at middle age in males followed by a decline at advanced age, whereas females showed no age-related changes in p-mTOR. Notably, females exhibited a progressive reduction in the p-mTOR/mTOR ratio with aging, while males maintained a relatively stable ratio across age groups. Together, the preservation of pAMPK/AMPK ratios across age and sex, despite pronounced sex- and age-dependent changes in p-mTOR, p-mTOR/mTOR, and ULK1Ser757 phosphorylation, suggests that autophagy impairment in htau mice is driven predominantly by AMPK-independent dysregulation of mTOR-ULK1 signaling, leading to sex-specific defects in late autophagy, altered autophagic flux, and differential accumulation of pathogenic tau species.

Correlation analysis. The observed sex-dependent differences in tau accumulation appear to align with distinct correlation patterns linking tau acetylation, total tau burden, acetyl-CoA metabolism, and protein clearance markers (**Figure 7, Supplementary Table 3D**). Across the dataset, TauK174ac tracked closely with Tau12 and with enzymes supporting acetylation capacity (e.g., ACSS2, CBP/p300), while showing inverse relationships with autophagy-related markers. These associations were not observed for phosphorylated tau species, which instead correlated more strongly with LAMP2A. Given that several of the acetylation- and autophagy-related proteins also exhibited sex-dependent expression or interactions

in two-way ANOVA analyses, the correlation structure is consistent with a sex-dependent coupling between tau acetylation and tau accumulation, rather than differences in tau phosphorylation per se. However, because these analyses are associative, they do not establish directionality or causality.

ARTICLE IN PRESS

Discussion

Dysfunctional tau protein is a hallmark neuropathology of AD. While A β can contribute to pathological misfolding of tau, evidence highlights the role of A β -independent tauopathy as a catalyst for neurodegeneration [14, 67], underscoring the central role of tau in AD etiology. Women are disproportionately diagnosed with AD, and studies suggest that females experience significantly greater tau burden than men with AD [68]. While abnormal phosphorylation of tau is believed to play a key role in pathological dysfunction, tau acetylation also promotes aggregation and may play a critical role in AD progression [12]. However, the sex-specific contributions of tau acetylation to the progression of tauopathy in AD and related diseases remains unclear. In this study, we examined the contribution of tau acetylation at lysine 174 site (TauK174ac), an early marker of tauopathy [30], to the sex-specific progression of A β -independent tauopathy.

Our results show that in htau mice, an A β -independent model of tauopathy, the age-dependent accumulation of TauK174ac in females is associated with tau oligomerization and accumulation without any significant changes in phosphorylation (AT8 and pTauTh231). Importantly, acetylation-related tau accumulation was specific to female htau mice, whereas male htau mice exhibited no changes in TauK174ac. These findings raise the possibility of sex-specific roles of PTMs, with TauK174 acetylation potentially contributing to tau oligomerization in female htau mice; however, future mechanistic studies will be required to confirm this role. While abnormally modified tau monomers can also be toxic, tau oligomers are considered among the most toxic tau species. Compared with physiological monomers or filamentous tau aggregates, as they induce greater synaptic and mitochondrial dysfunction in wild-type mice, ultimately leading to more severe memory deficits [69, 70]. In the transgenic PS19 mutant tau mouse model of tauopathy, TauK174ac colocalized with pathological tau paired helical filaments (PHFs) [21, 30]. Our findings in a humanized tauopathy mouse model demonstrate that phosphorylation-independent tau acetylation promotes tau oligomer accumulation and accelerates pathology in females.

Sex hormones and chromosomes can modulate AD progression by influencing processes such as inflammation, autophagy, and metabolism [71]. Protein acetylation integrates metabolic status with the regulation of gene expression, protein function, and proteostasis. In female htau mice, elevated TauK174 acetylation was observed despite unchanged expression of key metabolic enzymes involved in cytosolic acetyl-CoA production (ACLY and ACSS2) and NAD⁺-dependent deacetylation (Sirt1 and Sirt6), enzymes that critically regulate tau acetylation. This indicates that sex-specific differences in substrate metabolism are unlikely to explain the increased acetylation. Instead, the elevated TauK174ac levels were associated with upregulated expression of CBP/p300, lysine acetyltransferases known to acetylate tau. Both genetic and pharmacological inhibition of p300 in primary mouse neurons and brain tissue reduce total tau and TauK174ac levels [21]. Beyond their acetyltransferase activity, CBP/p300 act as co-activators of nuclear steroid hormone receptors, including androgen and estrogen receptors [72], suggesting that sex hormones may regulate CBP/p300 expression or activity via feedback mechanisms.

In contrast, aged male htau mice displayed significant increases in tau phosphorylation without a concomitant rise in TauK174 acetylation and oligomerization. These modifications of tau were accompanied by marked reductions

in ACLY expression, suggesting diminished cytosolic acetyl-CoA availability for acetylation. The unchanged CBP/p300 and Sirt1/Sirt6 expression levels further support the conclusion that limited acetyl-CoA supply, rather than altered enzyme expression, underlies the absence of age-associated TauK174ac elevation in males.

The precise role of TauK174ac in mediating sex-dependent tau oligomerization remains to be fully elucidated. However, acetylation at lysine 174, located within the proline-rich region (PRR) of tau, neutralizes the lysine's intrinsic positive charge, thereby diminishing electrostatic repulsion. This charge neutralization is proposed to lower the kinetic barrier for intermolecular interactions, facilitating tau self-association and aggregation [73]. Notably, females exhibit lower basal autophagic activity compared to males throughout the lifespan [74], which may contribute to impaired clearance of tau aggregates. This accumulation of tau aggregates can further suppress autophagy, creating a feed-forward loop that drives progressive neurodegenerative pathology [71]. Importantly, TauK174ac is associated with impaired tau degradation and reduced tau turnover, suggesting that acetylation at K174 may contribute to pathological tau accumulation by inhibiting its clearance [30]. Previous studies show that CBP/p300 not only promotes tau acetylation and accumulation [21] but also directly regulates autophagy by acetylating core autophagy proteins (Atg5, Atg7, Atg8, and Atg12), leading to p62 accumulation through suppression of autophagic flux at both initiation and degradation stages [75]. Consistent with these data, our studies demonstrate that the age-dependent increase in CBP/p300 expression and tau acetylation and oligomerization observed in female htau mice is accompanied by a marked reduction in autophagic activity. Specifically, we observed a significant decline in LC3-II levels, a key marker of autophagosome formation, in females but not in males, reinforcing the notion of sex-specific vulnerability. These findings align with emerging evidence implicating sex-dependent regulation of autophagy in AD and related tauopathies [76].

As a potential mechanism for sex-dependent autophagy alterations in htau mice, we examined AMPK and mTORC1 signaling, key regulators of tau phosphorylation and autophagy in AD and other tauopathies [77]. Under nutrient-deprived conditions, AMPK becomes activated, directly phosphorylates ULK1 at multiple sites, and promotes autophagy [64]. AMPK also regulates tau acetylation through Sirt1 activation. In contrast, mTOR inhibits autophagy by phosphorylating ULK1 at Ser757 [65]. Our findings suggest that aging induces a sex-dependent imbalance in AMPK/mTOR signaling, characterized by reduced AMPK activation and enhanced mTOR signaling in females, consistent with greater autophagy impairment. Simultaneous increased trend in ULK1 phosphorylation at serine 757 supports our interpretation that mTORC1 signaling inhibits autophagy, likely contributing to pathogenic tau accumulation in aged mice. Given the elevated CBP/p300 expression and their established roles in tau acetylation and acetylation-dependent autophagy regulation, our findings suggest that acetylation may further exacerbate this effect in females (**Figure 8**).

Despite providing novel insights into sex-specific associations among tau acetylation, autophagy, and tauopathy progression, several limitations should be considered when interpreting these findings. The primary limitation of this study is the relatively small sample size ($n = 4$ per group), which limits statistical power and reduces sensitivity to detect modest age- and sex-dependent effects across tau modifications and autophagy markers. Although changes in acetylated, total, and oligomeric tau,

as well as autophagy-related proteins, were internally consistent and mechanistically coherent, the limited cohort size restricts generalizability and precludes definitive causal inference. Notably, some potentially meaningful sex-specific age-related trends—such as those observed for TauK174ac, did not retain statistical significance following correction for multiple comparisons, likely reflecting insufficient power to detect interaction effects or subtle group differences. Accordingly, these findings should be regarded as hypothesis-generating and warrant validation in larger, independent cohorts to establish the robustness of the proposed sex-specific associations between tau acetylation, autophagy dysfunction, and tauopathy progression.

In conclusion, studies in htau mice reveal that age-related sex-specific impairments in autophagy, coupled with disruptions in brain acetylation, may be related to the progressive accumulation of tau pathology. Female mice appear particularly susceptible to acetylation-related dysregulation, autophagy deficits and promotion of tau abnormalities. These findings highlight acetylation as a key modulator of sex-dependent vulnerability and underscore the need for further investigation into acetylation-mediated mechanisms underlying tau pathology.

Data availability

The data supporting the findings of this study are available in Supplementary Materials. Supplementary Tables S1-S3 provide an overview of the datasets and protein-level summary statistics, and Supplementary Figures S1-S10 include immunohistology images and full-length representative immunoblots.

ARTICLE IN PRESS

References

1. Chandrashekar, D.V., et al., *Alcohol as a Modifiable Risk Factor for Alzheimer's Disease-Evidence from Experimental Studies*. Int J Mol Sci, 2023. **24**(11).
2. Sullivan, E.V. and A. Pfefferbaum, *Alcohol use disorder: Neuroimaging evidence for accelerated aging of brain morphology and hypothesized contribution to age-related dementia*. Alcohol, 2023. **107**: p. 44-55.
3. Bostrand, S.M.K., et al., *Associations between alcohol use and accelerated biological ageing*. Addict Biol, 2022. **27**(1): p. e13100.
4. Ferretti, M.T., et al., *Sex differences in Alzheimer disease - the gateway to precision medicine*. Nat Rev Neurol, 2018. **14**(8): p. 457-469.
5. Livingston, G., et al., *Dementia prevention, intervention, and care: 2024 report of the Lancet standing Commission*. Lancet, 2024. **404**(10452): p. 572-628.
6. Polanco, J.C., et al., *Amyloid-beta and tau complexity - towards improved biomarkers and targeted therapies*. Nat Rev Neurol, 2018. **14**(1): p. 22-39.
7. Bejanin, A., et al., *Tau pathology and neurodegeneration contribute to cognitive impairment in Alzheimer's disease*. Brain, 2017. **140**(12): p. 3286-3300.
8. Samudra, N., et al., *Tau pathology in neurodegenerative disease: disease mechanisms and therapeutic avenues*. J Clin Invest, 2023. **133**(12).
9. Cruz, E., et al., *Proteostasis as a fundamental principle of Tau immunotherapy*. Brain, 2025. **148**(1): p. 168-184.
10. Parra Bravo, C., S.A. Naguib, and L. Gan, *Cellular and pathological functions of tau*. Nat Rev Mol Cell Biol, 2024. **25**(11): p. 845-864.
11. Kyalu Ngoie Zola, N., et al., *Specific post-translational modifications of soluble tau protein distinguishes Alzheimer's disease and primary tauopathies*. Nat Commun, 2023. **14**(1): p. 3706.
12. Wesseling, H., et al., *Tau PTM Profiles Identify Patient Heterogeneity and Stages of Alzheimer's Disease*. Cell, 2020. **183**(6): p. 1699-1713 e13.
13. Goedert, M., et al., *Multiple isoforms of human microtubule-associated protein tau: sequences and localization in neurofibrillary tangles of Alzheimer's disease*. Neuron, 1989. **3**(4): p. 519-26.
14. Spillantini, M.G., et al., *Mutation in the tau gene in familial multiple system tauopathy with presenile dementia*. Proc Natl Acad Sci U S A, 1998. **95**(13): p. 7737-41.
15. Capano, L.S., et al., *Recapitulation of endogenous 4R tau expression and formation of insoluble tau in directly reprogrammed human neurons*. Cell Stem Cell, 2022. **29**(6): p. 918-932 e8.
16. Bachmann, S., et al., *Differential Effects of the Six Human TAU Isoforms: Somatic Retention of 2N-TAU and Increased Microtubule Number Induced by 4R-TAU*. Front Neurosci, 2021. **15**: p. 643115.

17. Lee, G., R.L. Neve, and K.S. Kosik, *The microtubule binding domain of tau protein*. *Neuron*, 1989. **2**(6): p. 1615-24.
18. Zheng, H., et al., *The Enigma of Tau Protein Aggregation: Mechanistic Insights and Future Challenges*. *Int J Mol Sci*, 2024. **25**(9).
19. Cook, C., et al., *Acetylation of the KXGS motifs in tau is a critical determinant in modulation of tau aggregation and clearance*. *Hum Mol Genet*, 2014. **23**(1): p. 104-16.
20. Cohen, T.J., et al., *The acetylation of tau inhibits its function and promotes pathological tau aggregation*. *Nat Commun*, 2011. **2**: p. 252.
21. Min, S.W., et al., *Acetylation of tau inhibits its degradation and contributes to tauopathy*. *Neuron*, 2010. **67**(6): p. 953-66.
22. Weaver, C.L., et al., *Conformational change as one of the earliest alterations of tau in Alzheimer's disease*. *Neurobiol Aging*, 2000. **21**(5): p. 719-27.
23. Gotz, J., et al., *What Renders TAU Toxic*. *Front Neurol*, 2013. **4**: p. 72.
24. Maeda, S., et al., *Increased levels of granular tau oligomers: an early sign of brain aging and Alzheimer's disease*. *Neurosci Res*, 2006. **54**(3): p. 197-201.
25. Combs, B., et al., *Frontotemporal Lobar Dementia Mutant Tau Impairs Axonal Transport through a Protein Phosphatase 1gamma-Dependent Mechanism*. *J Neurosci*, 2021. **41**(45): p. 9431-9451.
26. Rawat, P., et al., *Phosphorylated Tau in Alzheimer's Disease and Other Tauopathies*. *Int J Mol Sci*, 2022. **23**(21).
27. Giannakopoulos, P., et al., *Tangle and neuron numbers, but not amyloid load, predict cognitive status in Alzheimer's disease*. *Neurology*, 2003. **60**(9): p. 1495-500.
28. Hanger, D.P., B.H. Anderton, and W. Noble, *Tau phosphorylation: the therapeutic challenge for neurodegenerative disease*. *Trends Mol Med*, 2009. **15**(3): p. 112-9.
29. Fitzpatrick, A.W.P., et al., *Cryo-EM structures of tau filaments from Alzheimer's disease*. *Nature*, 2017. **547**(7662): p. 185-190.
30. Min, S.W., et al., *Critical role of acetylation in tau-mediated neurodegeneration and cognitive deficits*. *Nat Med*, 2015. **21**(10): p. 1154-62.
31. Kim, M.S., et al., *Tau acetylation at K280 regulates tau phosphorylation*. *Int J Neurosci*, 2023. **133**(12): p. 1394-1398.
32. Carlomagno, Y., et al., *An acetylation-phosphorylation switch that regulates tau aggregation propensity and function*. *J Biol Chem*, 2017. **292**(37): p. 15277-15286.
33. Julien, C., et al., *Sirtuin 1 reduction parallels the accumulation of tau in Alzheimer disease*. *J Neuropathol Exp Neurol*, 2009. **68**(1): p. 48-58.
34. Ding, H., P.J. Dolan, and G.V. Johnson, *Histone deacetylase 6 interacts with the microtubule-associated protein tau*. *J Neurochem*, 2008. **106**(5): p. 2119-30.
35. Tracy, T.E. and L. Gan, *Acetylated tau in Alzheimer's disease: An instigator of synaptic dysfunction underlying memory loss: Increased*

- levels of acetylated tau blocks the postsynaptic signaling required for plasticity and promotes memory deficits associated with tauopathy.* Bioessays, 2017. **39**(4).
36. Tracy, T.E., et al., *Acetylated Tau Obstructs KIBRA-Mediated Signaling in Synaptic Plasticity and Promotes Tauopathy-Related Memory Loss.* Neuron, 2016. **90**(2): p. 245-60.
 37. Shin, M.K., et al., *Reducing acetylated tau is neuroprotective in brain injury.* Cell, 2021. **184**(10): p. 2715-2732 e23.
 38. Duff, K., et al., *Characterization of pathology in transgenic mice over-expressing human genomic and cDNA tau transgenes.* Neurobiol Dis, 2000. **7**(2): p. 87-98.
 39. Tucker, K.L., M. Meyer, and Y.A. Barde, *Neurotrophins are required for nerve growth during development.* Nat Neurosci, 2001. **4**(1): p. 29-37.
 40. Combs, B., C. Hamel, and N.M. Kanaan, *Pathological conformations involving the amino terminus of tau occur early in Alzheimer's disease and are differentially detected by monoclonal antibodies.* Neurobiol Dis, 2016. **94**: p. 18-31.
 41. Horowitz, P.M., et al., *N-terminal fragments of tau inhibit full-length tau polymerization in vitro.* Biochemistry, 2006. **45**(42): p. 12859-66.
 42. Ward, S.M., et al., *TOC1: characterization of a selective oligomeric tau antibody.* J Alzheimers Dis, 2013. **37**(3): p. 593-602.
 43. Patterson, K.R., et al., *Characterization of prefibrillar Tau oligomers in vitro and in Alzheimer disease.* J Biol Chem, 2011. **286**(26): p. 23063-76.
 44. Ito, D., et al., *Microglia-specific localisation of a novel calcium binding protein, Iba1.* Brain Res Mol Brain Res, 1998. **57**(1): p. 1-9.
 45. Kanazawa, H., et al., *Macrophage/microglia-specific protein Iba1 enhances membrane ruffling and Rac activation via phospholipase C-gamma -dependent pathway.* J Biol Chem, 2002. **277**(22): p. 20026-32.
 46. Xia, Y., S. Prokop, and B.I. Giasson, *"Don't Phos Over Tau": recent developments in clinical biomarkers and therapies targeting tau phosphorylation in Alzheimer's disease and other tauopathies.* Mol Neurodegener, 2021. **16**(1): p. 37.
 47. Malia, T.J., et al., *Epitope mapping and structural basis for the recognition of phosphorylated tau by the anti-tau antibody AT8.* Proteins, 2016. **84**(4): p. 427-34.
 48. Dengler-Crish, C.M., M.A. Smith, and G.N. Wilson, *Early Evidence of Low Bone Density and Decreased Serotonergic Synthesis in the Dorsal Raphe of a Tauopathy Model of Alzheimer's Disease.* J Alzheimers Dis, 2017. **55**(4): p. 1605-1619.
 49. Wiera, G., et al., *Integrins Bidirectionally Regulate the Efficacy of Inhibitory Synaptic Transmission and Control GABAergic Plasticity.* J Neurosci, 2022. **42**(30): p. 5830-5842.
 50. Searle, S.R., F.M. Speed, and G.A. Milliken, *Population marginal means in the linear model: An alternative to least squares means.* The American Statistician, 1980. **34**(4): p. 216-221.

51. Lenth, R. and J. Piaskowski, *emmeans: Estimated Marginal Means, aka Least-Squares Means*. doi:10.32614/CRAN.package.emmeans <<https://doi.org/10.32614/CRAN.package.emmeans>>, 2025.
52. Andorfer, C., et al., *Hyperphosphorylation and aggregation of tau in mice expressing normal human tau isoforms*. J Neurochem, 2003. **86**(3): p. 582-90.
53. Covarrubias, A.J., et al., *NAD(+) metabolism and its roles in cellular processes during ageing*. Nat Rev Mol Cell Biol, 2021. **22**(2): p. 119-141.
54. Eftekhari, A., U. Sabir, and T. Kasumov, *The role of lysine acetylation in metabolic sensing and proteostasis*. Pharmacol Ther, 2025. **274**: p. 108908.
55. Lee, M.J., J.H. Lee, and D.C. Rubinsztein, *Tau degradation: the ubiquitin-proteasome system versus the autophagy-lysosome system*. Prog Neurobiol, 2013. **105**: p. 49-59.
56. Sadoul, K., et al., *Regulation of protein turnover by acetyltransferases and deacetylases*. Biochimie, 2008. **90**(2): p. 306-12.
57. Jahngen, J.H., et al., *Aging and cellular maturation cause changes in ubiquitin-eye lens protein conjugates*. Arch Biochem Biophys, 1990. **276**(1): p. 32-7.
58. Dudek, E.J., et al., *Ubiquitin proteasome pathway-mediated degradation of proteins: effects due to site-specific substrate deamidation*. Invest Ophthalmol Vis Sci, 2010. **51**(8): p. 4164-73.
59. Otda, T., et al., *Proteasome dysfunction mediates obesity-induced endoplasmic reticulum stress and insulin resistance in the liver*. Diabetes, 2013. **62**(3): p. 811-24.
60. Hara, T., et al., *Suppression of basal autophagy in neural cells causes neurodegenerative disease in mice*. Nature, 2006. **441**(7095): p. 885-9.
61. Russell, R.C., et al., *ULK1 induces autophagy by phosphorylating Beclin-1 and activating VPS34 lipid kinase*. Nat Cell Biol, 2013. **15**(7): p. 741-50.
62. Jung, C.H., et al., *ULK-Atg13-FIP200 complexes mediate mTOR signaling to the autophagy machinery*. Mol Biol Cell, 2009. **20**(7): p. 1992-2003.
63. Morita, T. and K. Sobue, *Specification of neuronal polarity regulated by local translation of CRMP2 and Tau via the mTOR-p70S6K pathway*. J Biol Chem, 2009. **284**(40): p. 27734-45.
64. Egan, D.F., et al., *Phosphorylation of ULK1 (hATG1) by AMP-activated protein kinase connects energy sensing to mitophagy*. Science, 2011. **331**(6016): p. 456-61.
65. Kim, J., et al., *AMPK and mTOR regulate autophagy through direct phosphorylation of Ulk1*. Nat Cell Biol, 2011. **13**(2): p. 132-41.
66. Shaw, R.J., et al., *The tumor suppressor LKB1 kinase directly activates AMP-activated kinase and regulates apoptosis in response to energy stress*. Proc Natl Acad Sci U S A, 2004. **101**(10): p. 3329-35.

67. Hutton, M., et al., *Association of missense and 5'-splice-site mutations in tau with the inherited dementia FTDP-17*. Nature, 1998. **393**(6686): p. 702-5.
68. Editorial, *2021 Alzheimer's disease facts and figures*. Alzheimers Dement, 2021. **17**(3): p. 327-406.
69. Lasagna-Reeves, C.A., et al., *Preparation and characterization of neurotoxic tau oligomers*. Biochemistry, 2010. **49**(47): p. 10039-41.
70. Lasagna-Reeves, C.A., et al., *Tau oligomers impair memory and induce synaptic and mitochondrial dysfunction in wild-type mice*. Mol Neurodegener, 2011. **6**: p. 39.
71. Lopez-Lee, C., et al., *Mechanisms of sex differences in Alzheimer's disease*. Neuron, 2024. **112**(8): p. 1208-1221.
72. Waddell, A.R., H. Huang, and D. Liao, *CBP/p300: Critical Co-Activators for Nuclear Steroid Hormone Receptors and Emerging Therapeutic Targets in Prostate and Breast Cancers*. Cancers (Basel), 2021. **13**(12).
73. Haj-Yahya, M. and H.A. Lashuel, *Protein Semisynthesis Provides Access to Tau Disease-Associated Post-translational Modifications (PTMs) and Paves the Way to Deciphering the Tau PTM Code in Health and Diseased States*. J Am Chem Soc, 2018. **140**(21): p. 6611-6621.
74. Shang, D., et al., *Sex differences in autophagy-mediated diseases: toward precision medicine*. Autophagy, 2021. **17**(5): p. 1065-1076.
75. Chen, X., et al., *Promoting tau secretion and propagation by hyperactive p300/CBP via autophagy-lysosomal pathway in tauopathy*. Mol Neurodegener, 2020. **15**(1): p. 2.
76. Congdon, E.E., *Sex Differences in Autophagy Contribute to Female Vulnerability in Alzheimer's Disease*. Front Neurosci, 2018. **12**: p. 372.
77. Caccamo, A., et al., *mTOR regulates tau phosphorylation and degradation: implications for Alzheimer's disease and other tauopathies*. Aging Cell, 2013. **12**(3): p. 370-80.

ACKNOWLEDGEMENTS

Funding: This work was supported in part by the National Institute of Health grants R21 AA029784 and 1R21AG085590-01 (T.K.), RF1 NS082730 (NK) and an Alzheimer's Association ALZDISCOVERY-1052089 grant (C.M.D.C.). We thank Dr. Adam Grden and Sameer Parashar for their technical assistance.

Author contributions: Conceptualization: T.K. and C.M.D.C. Methodology: U.S, B.A.C., S.I., Y.A., N.K., Formal Analysis: U.S., T.-H.T., S.I., Visualization: T.-H.T., S.U., C.M.D.C., Supervision: T.K., and C.M.D.C., Writing: T.K., Review and editing: S.U., B.A.C., S.I., Y.A., N.K., T.-H.T., D.S., C.M.D.C., and T.K.

Competing interests: All authors declared that there are no conflicts of interest.

ARTICLE IN PRESS

Figure legends.

Figure 1. Immunofluorescent staining for acetylated tau (K174ac) and phosphorylated tau (AT8 tau) in fixed coronal sections of hippocampal dentate gyrus (DGpo) hemifields of aged (19-month-old symptomatic) htau mice. Top micrographs: Left: K174ac (red); middle: pTauS202/T205 (AT8 antibody, blue); right: merged channel images. Magnified views show increased pTau in both sexes, elevated K174ac only in females, and greater overlap of signal in females. No signal above background was detected in age- and sex-matched tau^{-/-} controls. Orthogonal plots of z-stack images from hippocampal hemifields of 19-month-old htau mice showing co-expression of acetylated and phosphorylated tau are showing in supplementary Figure 1. Scale bar = 50 μm. Bottom bar graphs: quantified data from micrographs showing integrated fluorescent density of acetylated tau (left) and ptau202 (middle) in htau hippocampus, indicating elevated levels in female htau mice relative to males. Left: Manders coefficient data show significantly more colabel between acetylated tau and ptau202 in female htau mice compared to their male counterparts. Asterisk indicates $p < 0.05$. Quantified data are not provided for tau^{-/-} as measurements are not detectable above background.

Figure 2. Microglial activation is increased in aged female htau brain and coincides with upregulated acetylated tau. Multichannel immunofluorescence micrographs (columns 1 and 3) depict colabeled acetylated tau (K174ac) and phosphorylated tau (AT8 tau); single-channel images (columns 2 and 4) show Iba1+ microglia in 16-19 months old female (left panel) and male (right panel) htau mice hippocampal (DGpo) hemifields. Images correspond to the sections for female and male htau mice shown in Fig. 1. Scale bars = 50 μm.

Figure 3. Age-related changes in tau acetylation, phosphorylation, and oligomerization in the prefrontal cortex (PFC) of female and male htau mice. (A, B) Western blot analysis of total tau (Tau12), phosphorylated tau (AT8, Thr231), and acetylated tau (K174) in female and male htau mice at three ages: pre-symptomatic (3-5 months), progressive stage (11-14 months), and advanced stage (>16 months) (n = 4 per group). Tau acetylation (K174ac) increased with age in females, while tau phosphorylation at S202/T205 (AT8 tau) increased in males; tau aggregation was elevated in both sexes. Actin served as a loading control, and data were normalized to actin levels. Full versions of the representative blots are shown in supplementary **Figures S3A-E**.

(D, E) Dot blot analysis of total tau and tau oligomers using the Tau12 and TOC1 antibodies in female and male htau mice across the three age groups (n = 4 per group). TOC1 signals were quantified and normalized to total tau levels and expressed as the ratio of TOC1 to total tau.

(C, F) Bar graphs show the estimated marginal mean ± standard error of expression levels for each sex-age group, with individual data points representing measurements from single animals. The subtitle reports the p-values for the main effect of age and the sex × age interaction derived from the two-way ANOVA. When a significant interaction was detected, post hoc interaction analyses were performed; to avoid visual clutter, only significant pairwise age contrasts after Bonferroni correction are shown (adjusted * $p < 0.05$, ** $p < 0.005$, *** $p < 0.001$). When the interaction was not significant, the main effect of age was evaluated, and if significant ($p < 0.05$), post hoc comparisons among the three age groups were conducted while collapsing across

sex. In this case, a dashed line connecting the two sex levels indicates that sex was not included in the post hoc age comparisons.

Figure 4. Age-dependent regulation of acetylation in the htau mice. A: Schematic illustrating the molecular mechanisms regulating protein acetylation in the nucleus and cytosol. Substrate metabolism in mitochondria produces acetyl-CoA, fueling tau acetylation. Acetyl-CoA is exported to the nucleus or cytoplasm via citrate or acetyl-carnitine (CrAT), where citrate is reconverted by ATP-citrate lyase (ACLY). Free acetate also generates nuclear-cytosolic acetyl-CoA via acetyl-CoA synthetase 2 (ACSS2). Lysine acetyltransferases (KATs; e.g., CBP/p300 and NAD⁺-dependent deacetylases (Sirt1/6) dynamically regulate tau acetylation.

Western blot analysis of lysine acetyl transferase (KAT; **B, C**), NAD⁺-dependent deacetylases (sirtuins; **D, E**), and enzymes involved in nuclear-cytosolic acetyl-CoA synthesis (**F, G**) was performed in the prefrontal cortex of female and male htau mice across three age groups: pre-symptomatic (3–5 months), progressive disease (11–14 months), and advanced disease (>16 months) (n=4 mice per group). Actin was used as the loading control for protein normalization. Full versions of the representative blots are shown in **Supplementary Figures S4A-H**.

(**H**) Bar graphs show the estimated marginal mean \pm standard error of expression levels for each sex-age group, with individual data points representing measurements from single animals. The subtitle reports the p-values for the main effect of age and the sex \times age interaction derived from the two-way ANOVA. When a significant interaction was detected, post hoc interaction analyses were performed; only significant pairwise age contrasts after Bonferroni correction are shown (adjusted $*p < 0.05$, $**p < 0.005$, $***p < 0.001$). When the interaction was not significant, the main effect of age was evaluated, and if significant ($p < 0.05$), post hoc comparisons among the three age groups were conducted while collapsing across sex.

Figure 5. Impaired autophagy in female and male htau mice. (A) Schematic of dysfunctional autophagy in tauopathy (created with BioRender.com).

Western blot analysis of autophagy markers related to initiation, lipidation, maturation and chaperone-mediated autophagy was performed in the prefrontal cortex of male (**B, E, and H**) female (**C, F, and I**) htau mice at pre-symptomatic (3–5 months), progressive (11–14 months), and advanced (>16 months) stages (n=4 mice per group). Actin was used for protein normalization. In females, advanced age was associated with reduced LC3-II, indicating impaired autophagic flux and compromised autophagosome biogenesis.

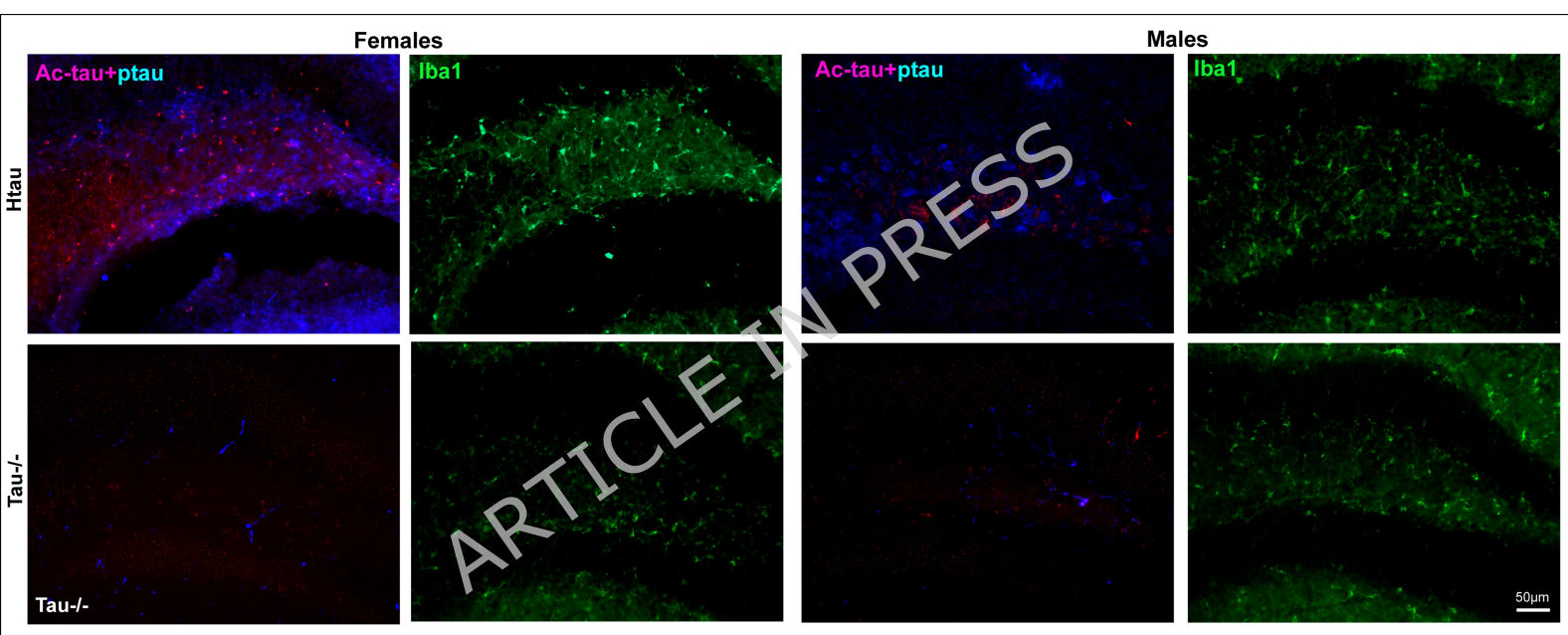
(**D, G, J**) Bar graphs show the estimated marginal mean \pm standard error of expression levels for each sex-age group, with individual data points representing measurements from single animals. The subtitle reports the p -values for the main effect of age and the sex \times age interaction derived from the two-way ANOVA. When a significant interaction was detected, post hoc interaction analyses were performed; only significant pairwise age contrasts after Bonferroni correction are shown (adjusted $*p < 0.05$, $**p < 0.005$, $***p < 0.001$). When the interaction was not significant, the main effect of age was evaluated, and if significant ($p < 0.05$), post hoc comparisons among the three age groups were conducted while collapsing across sex. In this case, a dashed line connecting the two sex levels indicates that sex was not included in the post hoc age comparisons.

Full versions of the representative blots are shown in **Supplementary Figures S8A-J**.

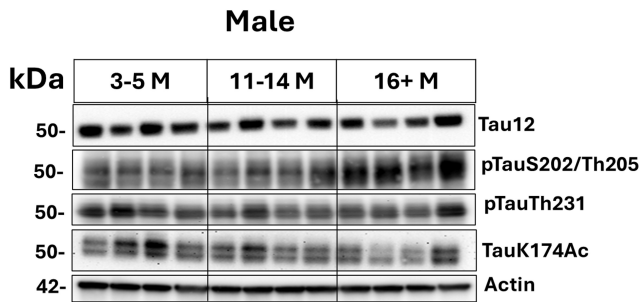
Figure 6. Role of mTOR in age-dependent and sex-specific tauopathy in htau mice. Western blot analysis of total mTOR and phosphorylated mTOR (Ser2448) in prefrontal cortex (PFC) region of three age groups of females (**A**) and male (**B**) htau mice, comprised of pre-symptomatic (3-5 months old); progressive-disease stage (11-14 months old) and advanced-disease stage (>16 months old), (n=4 mice per group). **(C)** Bar graphs show the estimated marginal mean \pm standard error of expression levels for each sex-age group, with individual data points representing measurements from single animals. The subtitle reports the p -values for the main effect of age and the sex \times age interaction derived from the two-way ANOVA. When a significant interaction was detected, post hoc interaction analyses were performed; only significant pairwise age contrasts after Bonferroni correction are shown (adjusted $*p < 0.05$, $**p < 0.005$, $***p < 0.001$). When the interaction was not significant, the main effect of age was evaluated, and if significant ($p < 0.05$), post hoc comparisons among the three age groups were conducted while collapsing across sex. In this case, a dashed line connecting the two sex levels indicates that sex was not included in the post hoc age comparisons. Full versions of the representative blots are shown in **Supplementary Figures S10A-H**.

Figure 7. Correlation matrix of all quantified markers. Pearson correlation coefficients (r) are displayed as a heatmap, with color intensity and direction indicating the strength and sign of the correlations, as shown in the scale bar on the right. Statistically significant correlations are annotated according to their p -values ($*p < 0.05$, $**p < 0.005$, $***p < 0.001$).

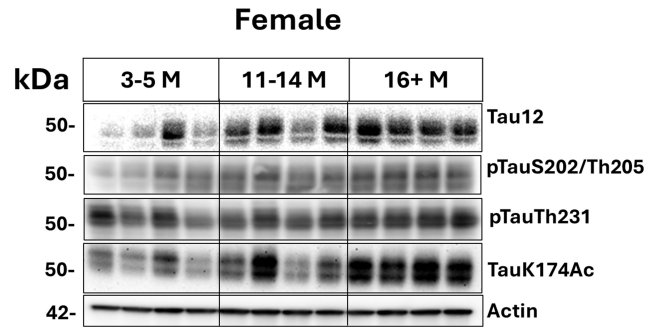
Figure 8. Proposed model: sex-dependent tau phosphorylation, acetylation, and mTOR signaling impair tau degradation and promote oligomerization. With aging, increased tau phosphorylation in males and elevated tau acetylation in females, together with aging-associated mTOR activation, converge to suppress autophagy-mediated tau clearance. Impaired degradation promotes tau oligomer formation, thereby accelerating tauopathy progression in a sex-dependent manner.



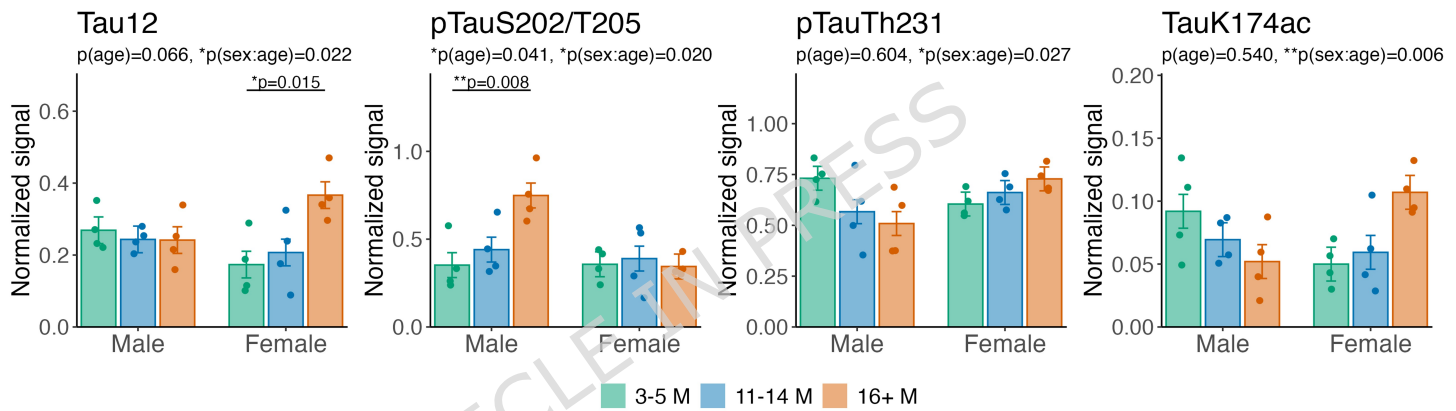
A



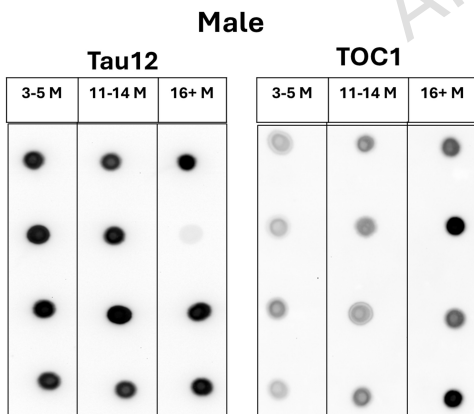
B



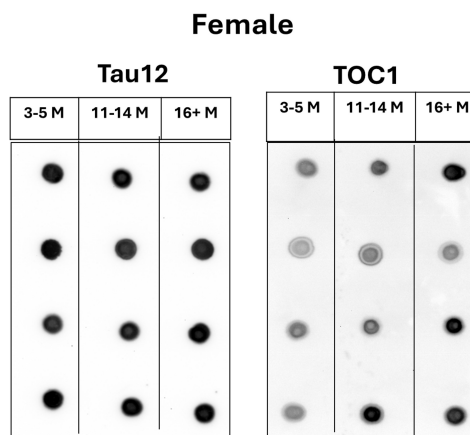
C



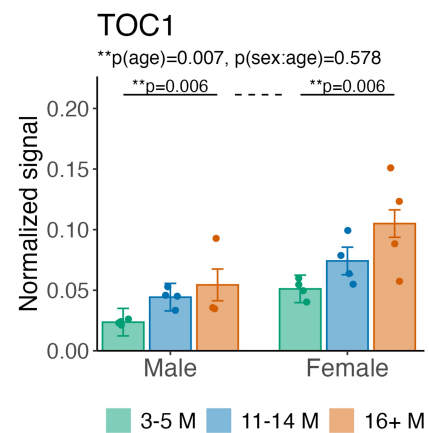
D



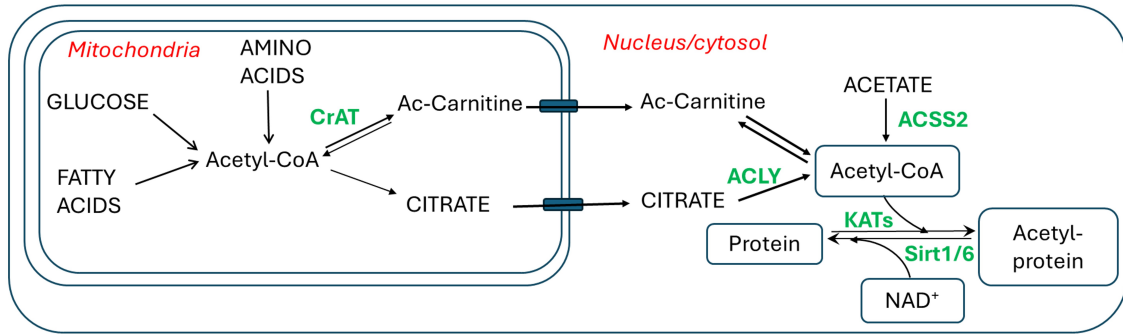
E



F

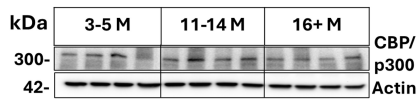


A



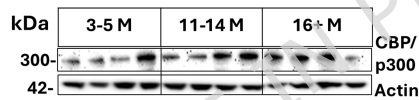
B

Male

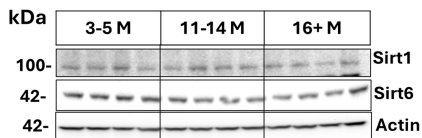


C

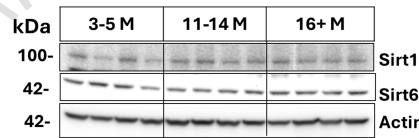
Female



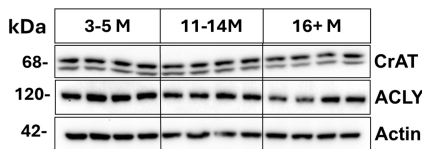
D



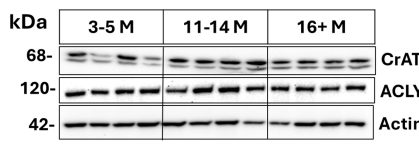
E



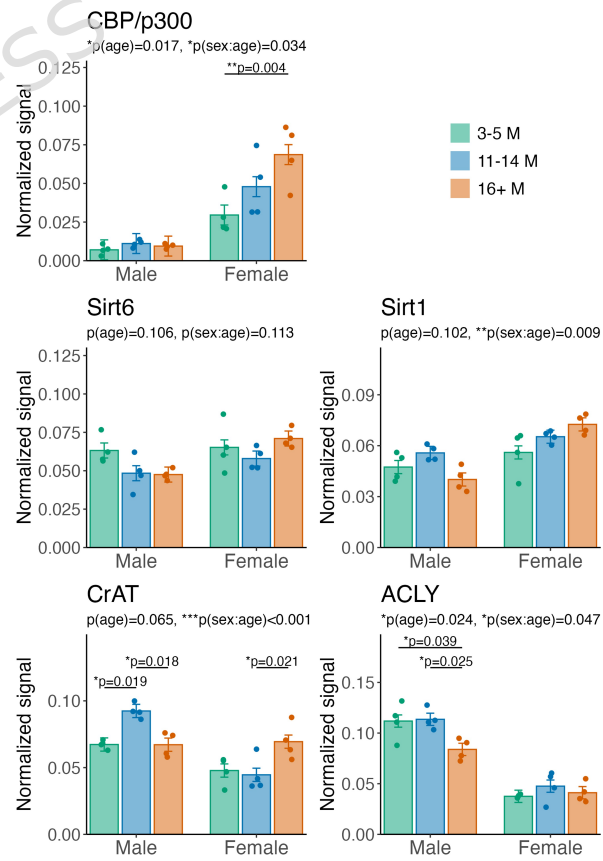
F

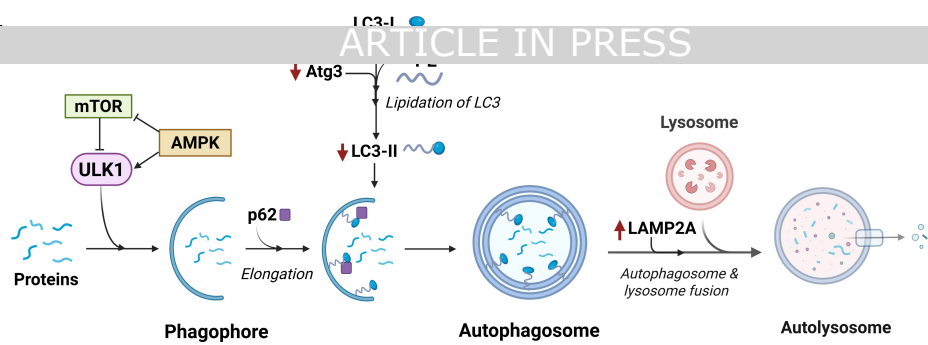


G

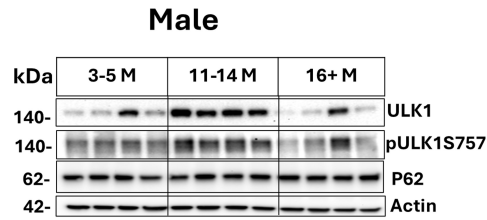


H

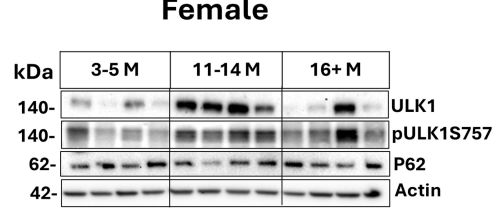




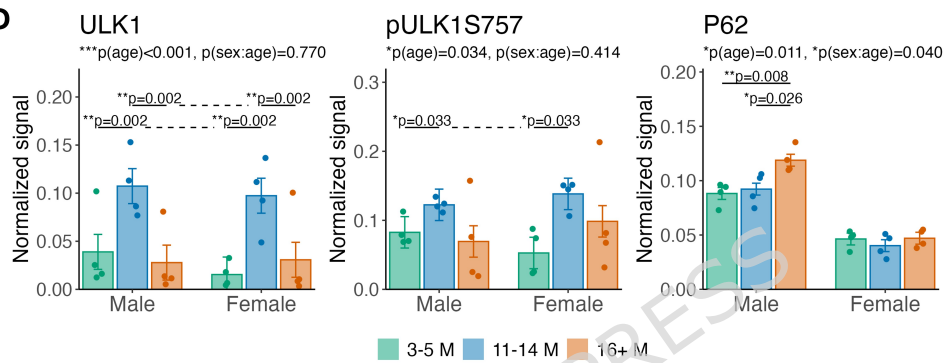
B



C



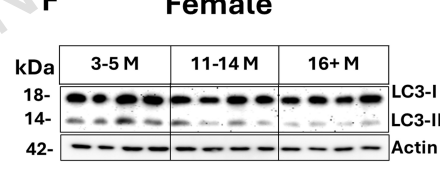
D



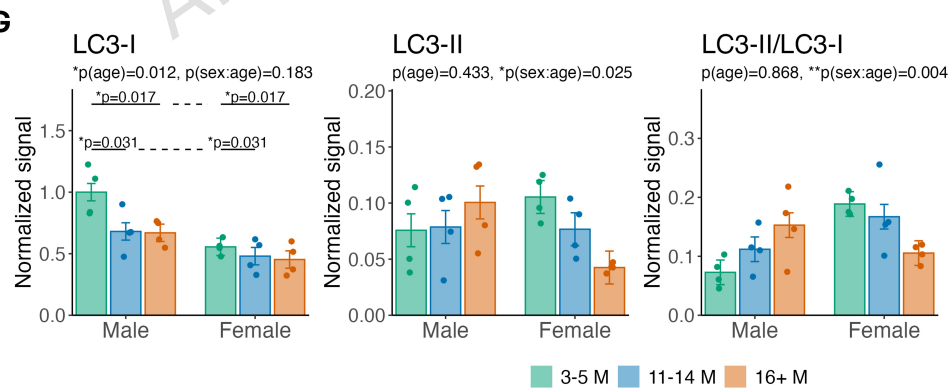
E



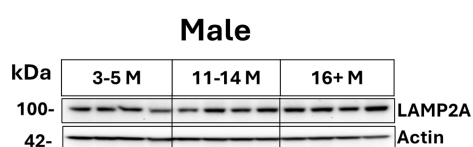
F



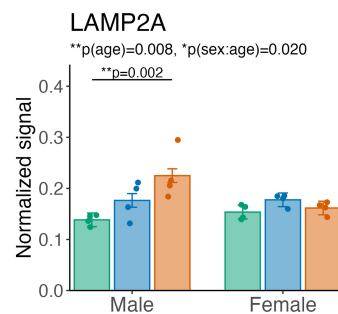
G



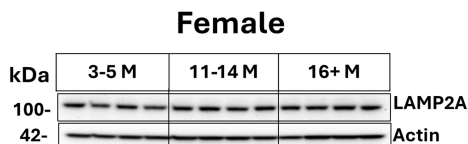
H



J



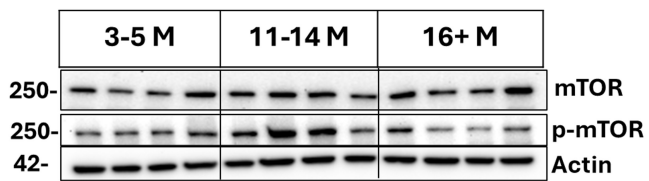
I



3-5 M 11-14 M 16+ M

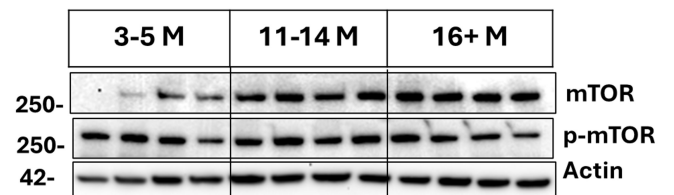
A

Male



B

Female



C

